

Generalized Kitaev Spin Liquid model and Emergent Twist Defect

Bowen Yan ^{*1}, Penghua Chen¹, and Shawn X. Cui ^{*1,2}

¹Department of Physics and Astronomy, Purdue University, West Lafayette

²Department of Mathematics, Purdue University, West Lafayette

{yan312, chen3014, cui177} @purdue.edu

Abstract

The Kitaev spin liquid model on honeycomb lattice offers an intriguing feature that encapsulates both Abelian and non-Abelian phases[1]. Recent studies suggest that the comprehensive phase diagram of possible generalized Kitaev model largely depends on the specific details of the discrete lattice, which somewhat deviates from the traditional understanding of “topological” phases. In this paper, we propose an adapted version of the Kitaev spin liquid model on arbitrary planar lattices. Our revised model recovers the surface code model under certain parameter selections within the Hamiltonian terms. Changes in parameters can initiate the emergence of holes, domain walls, or twist defects. Notably, the twist defect, which presents as a lattice dislocation defect, exhibits non-Abelian braiding statistics upon tuning the coefficients of the Hamiltonian. Additionally, we illustrate that the creation, movement, and fusion of these defects can be accomplished through natural time evolution by linearly interpolating the static Hamiltonian. These defects demonstrate the Ising anyon fusion rule as anticipated. Our findings hint at possible implementation in actual physical materials owing to a more realistically achievable two-body interaction.

1 Introduction

Since Kitaev proposed the Kitaev Quantum Double model[2], it has garnered considerable attention due to its typical anyon behavior and the paradigm it provides for topological quantum computation. The model demonstrates how one can circumvent local errors by encoding information into anyon types and executing gates through anyon braiding, whose information is completely described by Unitary Modular Tensor Categories (UMTC). It has been proven

*Corresponding author

that certain non-Abelian cases, such as Fibonacci Anyon, can support universal quantum computation.

Following this development, numerous lattice models have been proposed with the objective of identifying different types of anyons. Two significant classes of these include the Kitaev Quantum Double model[2] and the Levin-Wen model[3]. These models actualize anyon models from varying perspectives, which are described by the Drinfeld center of a fusion category.

The realization of the actual topological phase is a complex and pivotal task. Renowned models, such as the Kitaev Quantum Double model and Levin-Wen model, necessitate multi-body interactions, making them challenging to implement in a real-world laboratory setting. While some comparatively achievable cases, such as the toric code, are not suitable for universal computation because it only supports Abelian anyons. This reality has led to an increased interest in the twist defect, as introduced by [4]. This defect exemplifies a non-Abelian Ising anyon, which stems from the lattice dislocation of, the Abelian anyon case, the toric code model. Recent experimental observations of the Ising anyon statistics, as reported by [5], attest to this. It should be noted that the defect is dependent on the disruption of the lattice's local two-colorability.

Another intriguing model is the Kitaev spin liquid Model[1], which supports Abelian anyons in the gapped phase region, as well as non-Abelian anyons upon the introduction of a magnetic field to the gapless phase. This model is simple yet fruitful. But the definition of the model relies heavily on the geometry of honeycomb lattice, which deviates the idea of topological phase and is the main question to be solved in this paper. Moreover, it also has been pointed out that a spin liquid model on honeycomb lattice with lattice dislocation will generate the twist defect as in [6]. The generalization to Zetor model has been shown in [7]. This model is potentially easily realizable in a real laboratory due to the two-body nearest interaction.

Considerable theoretical progress has been made in the generalization of this model. Examples include those on a translationally invariant two dimensional lattice with higher-coordination vertices [8][9][10], on a two-dimensional amorphous lattice [11], a three-dimensional diamond lattice [12], and works on trivalent 3D lattices [13]. It is clear that the overall phase diagram is strongly influenced by the geometric specifics of the lattice, thus also deviating our traditional understanding of 'topological' phases.

In this paper, we demonstrate that the entire theory can be formulated on a generic planar lattice. The main motivation relies on the toric code limit of the original honeycomb spin liquid model as mentioned before, which is briefly reviewed in section(2). We sketch the main idea here and details are in the following sections.

The Hamiltonian of the honeycomb spin liquid system is a summation of weighted check operators, which are two-body nearest Pauli operators. The Hamiltonian is frustrated due to non-commutation of the check operators. We say a check operator in the Hamiltonian is dominant if the coefficient of the operator is much larger than others. Kitaev selected what he refers to as "z-link" check operators to take dominance in the Hamiltonian. As a result, the

vicinity of the ground state in the spectrum can be accurately described by a toric code model. The exact choice of “z-link” check operators is not important. The key is that “z-link” check operators composite a maximum set of commuting operators, which is denoted as **stabilizer center** S_c in this paper. S_c satisfies that any check operator outside this set should anticommutes with exactly two elements in S_c . We find that if one can find a proper S_c on an arbitrary planar lattice, a toric code model always appears in the vicinity of the ground state, provided all elements in the S_c are dominant.

Moreover, we get toric code with defects if we slight break the requirement of S_c . Further, we propose that a linear interpolating Hamiltonians, which statically has different dominant S_c s, could be a natural way to create, move, and fuse defects in a physical system. This approach circumvents the need for geometric deformation or the application of a coding method. This proposal might inspire real material realization since we only need to establish and adjust the strength of two-body interactions, as illustrated in section 4. Moreover, a circuit description is plausible since these operations are facilitated by time evolution operators, which are naturally unitary.

This paper is organized as follows:

In Section 2, we provide a concise review of the original honeycomb model and reintroduce necessary notations, such as the shrunken lattice.

Section 3 introduces our method of generalization. Initially, we rewrite the toric code on a lattice where qubits are positioned on vertices instead of edges, as discussed in Section 3.1. This rewriting is inspiring since the recovery of toric code typically ends in a lattice where qubits are placed on vertices. Subsequently, in Sections 3.2 and 3.3, we demonstrate how to define check operators on arbitrary lattices and, given an appropriate choice of a Stabilizer Center (S_c), the toric code can be recovered when the shrunken lattice is 2-colorable. We should note that a local disruption of the two-colorability of the shrunken lattice leads to the emergence of a twist defect.

Section 4 illustrates the process of creation, movement, and fusion of defects through time evolution operators.

Next, in Section 5, we demonstrate that the entire model can be treated as a zero-logic-qubit subsystem code in the context of error correcting code.

Finally, Section 6 concludes the paper and discusses potential future extensions.

2 Kitaev Honeycomb Model

Let us briefly revisit the Kitaev Honeycomb Model and establish some notations. The lattice, depicted in Figure 1a and denoted by $\Gamma = (V, E, P)$, consists of vertices (V), edges (E), and plaquettes (P).

The notation $\partial_1 e$, $\partial_2 e$ is used to refer to the two vertices at the end of edge $e \in E$, and $\partial e = \{\partial_1 e, \partial_2 e\}$ indicates the set. $N(A)$ is the count of the set A . A frequently used symbol d_v denotes the count of set $e|e \in E, v \in \partial e$, i.e., the

degree of the vertex v . $Bo(p) \subseteq E$, for $p \in P$ represents the edges that border the plaquette p .

Each vertex houses a qubit. The total Hilbert Space is:

$$\mathcal{H} := \bigotimes_{e \in E} \mathcal{H}_e \quad (1)$$

Each edge on the lattice is associated with a symbol x, y, z . For the honeycomb lattice, we label all the edges as illustrated in Figure 1a, consistent with the original paper[1]. These edges are referred to as “x-edges”, “y-edges”, and “z-edges”. The edge associated with $x(y, z)$ involves a two-body Pauli operator $X \otimes X (Y \otimes Y, Z \otimes Z)$ acting on the qubits at the ends of the edge. The operators linked to edges are defined as check operators, denoted by P_e . We say that two check operators are unconnected if the edges associated with these operators are not connected. In this paper, we use X, Y, Z to represent Pauli Operators $\sigma_x, \sigma_y, \sigma_z$:

$$\sigma_x = \begin{pmatrix} 0 & 1 \\ 1 & 0 \end{pmatrix}, \quad \sigma_y = \begin{pmatrix} 0 & -i \\ i & 0 \end{pmatrix}, \quad \sigma_z = \begin{pmatrix} 1 & 0 \\ 0 & -1 \end{pmatrix}$$

The Hamiltonian is the summation of weighted check operators:

$$H = -J_x \sum_{x\text{-edges}} X \otimes X - J_y \sum_{y\text{-edges}} Y \otimes Y - J_z \sum_{z\text{-edges}} Z \otimes Z \quad (2)$$

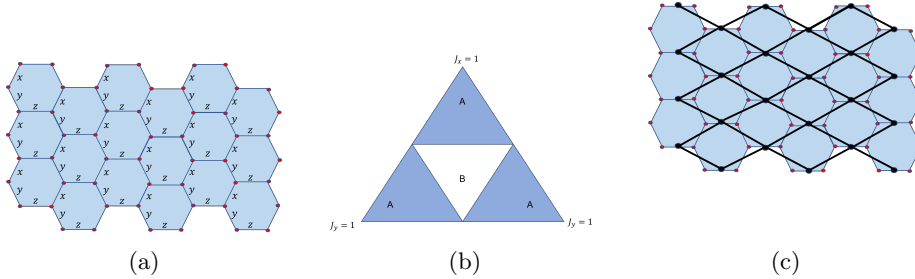


Figure 1: (a) Figure 1: The original Honeycomb Lattice.(b) Figure 2: Phase diagram depicting the gapped phases. When one of J_x, J_y , or J_z is dominant, it is mathematically equivalent to a toric code model. (c) Figure 3: Depiction of the shrunken lattice when J_z is dominant, illustrated by the reduction of two physical qubits to one effective qubit in the ground state of the “z-edge” check operators.

As depicted in Figure 1b, the phase diagram of the Honeycomb model is well-defined. In the $A(B)$ region, it represents a gapped(gapless) phase. Kitaev explicitly demonstrated, using perturbation theory, that the gapped phase is the toric code phase, where one of the J_x, J_y, J_z variables is much larger than others. Then those two qubits connected by z - edges will stay at the ground state of

the check operator $Z \otimes Z$. We say these two qubits are effectively “shrunk” to a single qubit. Subsequently, the lattice is also shrunk by replacing the edge to a single vertex, as shown in Figure 1c. This is referred to as the “shrunk” lattice.

Let us rephrase this in our notations. We denote these check operators associated with $z - edges$ as a Stabilizer center S_c . We obtain a shrunk lattice when this S_c is dominant. The ground state under this limit is twofold: it is simultaneously the ground state of S_c and the ground state of all plaquette terms W_p , where W_p is the product of check operators associated to edges in $Bo(p)$.

Generally, on a trivalent lattice, a Hamiltonian of the following form can be considered:

$$H = - \sum_{e \in E} J_e P_e \quad (3)$$

The definition of check operators could be varied as long as the following commutative relation remains:

$$[P_e, P_{e'}] = 0 \text{ if } \partial e \cap \partial e' = \emptyset \quad (4)$$

$$\{P_e, P_{e'}\} = 0 \text{ if } \partial e \cap \partial e' \neq \emptyset \quad (5)$$

$$(6)$$

For any $e \neq e'$. This means that check operators should anticommute if they intersect at exactly one vertex and commute in other scenarios. We require all check operators in S_c to be unconnected. When we allow S_c to be dominant, we obtain a shrunk lattice by replacing the edges of S_c by a single vertex. We will demonstrate that this will be a specific surface code. Indeed, the shrunk lattice at different S_c may vary. In this honeycomb lattice, the shrunk lattice at dominant $x - edges$ and $z - edges$ are all square lattices. However, in [14], their shrunk lattice is a kagome lattice (when the qubits are considered to be placed on vertices). We will frequently utilize the concept of a shrunk lattice at a given S_c .

3 Generalized Method

3.1 Toric Code on a lattice where qubits are placed on vertices

The toric code model is defined on an arbitrary planar lattice $\Gamma = (V, E, P)$, with one qubit placed on each edge. The Hamiltonian is:

$$H = - \sum_v A_v - \sum_p B_p \quad (7)$$

Here, $A_v = \bigotimes_{e|v \in \partial e} X_e$ and similarly, $B_p = \bigotimes_{e|e \in Bo(p)} Z_e$. The symbols X_e and Z_e indicate that the Pauli operator X and Z acts on the qubit placed on the edge e . For our purposes, we need to reshape the lattice into a more convenient

form as shown in figure 2. The process is as follows. First, we attach a new vertex on each edge e , denoted by red dots. We add one edge to connect red dots on e_1 and e_2 if they satisfy:

$$e_1 \neq e_2 \quad (8)$$

$$N(\partial e_1 \cap \partial e_2) = 1 \quad (9)$$

$$\exists p \in P, e_1, e_2 \subseteq Bo(p) \quad (10)$$

We will add two edges to connect e_1 and e_2 if $N(\partial e_1 \cap \partial e_2) = 2$ in the above requirement. This results in a new lattice $\Gamma' = (V', E', P')$, where V' is the set of red dots and $V' = E$ as sets. E' is the set of newly added edges connecting red dots and $P' = V \cup P$ as sets.

Notably, the degree of the new vertex is automatically 4. The new plaquettes are two-colored by vertices and plaquettes of Γ . Consequently, the toric code becomes a lattice model on Γ' , with one qubit placed on each vertex. In the new lattice as in figure 2c, the plaquette $p_g(p_r)$ with a green(red) circle has a plaquette term that is $\otimes X(Z)$ on each qubit on the boundary of $p_g(p_r)$, corresponding to previous $A_v(B_p)$ operators.

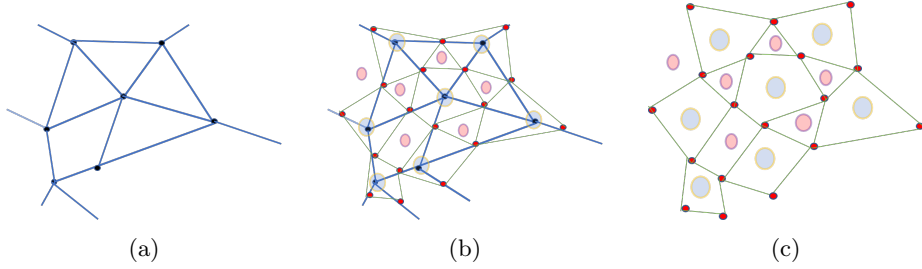


Figure 2: (a) Figure 1: Original lattice model with qubits placed on edges. Black dots represent vertices E .(b) Figure 2: Transformation process of the lattice. Red dots label the center of edges. Two red dots are connected if they belong to the same plaquette and are connected. New plaquettes are colored in red and grey circles.(c) Figure 3: The transformed lattice with qubits on vertices. And the original lattice is removed. A_v and B_p operators act on the two types of plaquettes, labeled by red and grey circles respectively.

3.2 Generalized model on a lattice with all vertices having even degree

Begin with a lattice $\Gamma = (V, E, P)$, where each vertex $v \in V$ has an even degree d_v . Our purpose is to define check operators and ensure the Hamiltonian remains the weighted summation of these check operators. The check operator P_e should take a form that is a tensor product of Pauli operators acting on the ends of edge e , namely $P_e = P_{\partial_1 e} \otimes P_{\partial_2 e}$. To maintain the property that check operators anticommute if they are connected, we require additional operators

that anticommute with each other when the vertex has a higher degree. We find that placing $d_v/2 - 1$ qubits on each vertex facilitates this. For k qubits, we have $2k + 1$ mutually anti-commuting Pauli operators as follows:

$$\begin{aligned}
p_1 &= 1 \otimes 1 \otimes 1 \otimes \cdots X \\
p_2 &= 1 \otimes 1 \otimes 1 \otimes \cdots Y \\
&\vdots \\
p_{2t+1} &= \underbrace{1 \cdots 1}_{k-t-1} \otimes X \otimes Z \otimes \cdots Z \\
p_{2t+2} &= \underbrace{1 \cdots 1}_{k-t-1} \otimes Y \otimes Z \otimes \cdots Z \\
&\vdots \\
P_{2k+1} &= Z \otimes Z \otimes Z \otimes \cdots Z
\end{aligned} \tag{11}$$

Importantly, because we ultimately aim to reach the toric code, the signs of each term do not significantly matter, as different sign configurations are related by unitary transformations. This allows us to consider each operator within the Pauli group $\mathcal{P} = \{G/\{+1, -1, +i, -i\}\}$, where G is designated to represent the set of all possible tensor products of Pauli operators.

Within the Pauli group, the phase gate P_{gate} interchanges X and Y , while leaving Z unaffected. This can swap P_{2t+1} with P_{2t+2} for any $0 \leq t < k$. Subsequently, the Hadamard gate H_{gate} flips X and Z , which in turn flips P_{2k+1} with P_{2k-1} . The gate $S_{\text{gate}} = P_{\text{gate}} \circ H_{\text{gate}} \circ P_{\text{gate}}$ flips Y and Z . CNOT gate is a unitary operator. Elementary actions by conjugating CNOT gate on two-qubits Pauli operators are given by:

$$\begin{aligned}
\text{CNOT}(IX) &= IX, & \text{CNOT}(XI) &= XX, \\
\text{CNOT}(IZ) &= ZZ, & \text{CNOT}(ZI) &= ZI.
\end{aligned} \tag{12}$$

A sequence of conjugations of operators above is then sufficient to flip P_1 with P_4 , noting that it is sufficient to consider only the last two qubits. Here is how to flip $X \otimes Z$ with $1 \otimes Y$, without changing the other operators:

$$\begin{array}{ccccccc}
X \otimes Z & \xrightarrow{H_{\text{gate}} \otimes \text{Id}} & Z \otimes Z & \xrightarrow{\text{CNOT}} & 1 \otimes Z & \xrightarrow{S_{\text{gate}} \otimes S_{\text{gate}}} & 1 \otimes Y & \xrightarrow{P_{\text{gate}} \otimes 1} & 1 \otimes Y \\
1 \otimes Y & \xrightarrow{H_{\text{gate}} \otimes \text{Id}} & 1 \otimes Y & \xrightarrow{\text{CNOT}} & Z \otimes Y & \xrightarrow{S_{\text{gate}} \otimes S_{\text{gate}}} & Y \otimes Z & \xrightarrow{P_{\text{gate}} \otimes 1} & X \otimes Z
\end{array}$$

This approach is sufficient to exchange any P_i with P_j by stacking the aforementioned operations, asserting that any distribution of these operators is equivalent. Consider a lattice where all vertices have a degree of four. The check operator on an edge, P_e , can be defined as the tensor product of Pauli operators supported on the vertices at the end of the edge e . It is important to note that the actual assignment of a Pauli operator for one P_e is not crucial, as long as P_e operators anticommute with each other when they are connected. Figure 3 provides an example of the assignment of Pauli operators, and any other assignment is equivalent up to a unitary transformation. An operator P_v represents

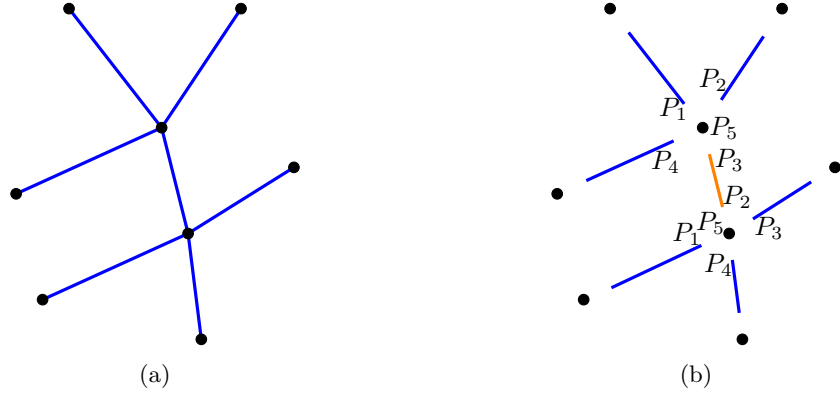


Figure 3: (a) Figure 1: A local part of the entire lattice diagram. (b) Figure 2: A simplified illustration of the assignment of Pauli operator P_1 through P_4 from each vertex v to the surrounding P_e , while P_5 is assigned to the P_v . Each P_e is the tensor product of operators from the two end vertices of e . For example, the operator on the orange edge is $(1 \otimes X) \otimes (Y \otimes Z)$, or simply $P_3 \otimes P_2$.

a new type of check operator that is associated with only one vertex v , which, for our convenience, is chosen as $P_v = P_5$. The Hamiltonian is as follows:

$$H = - \sum_v J_v P_v - \sum_e J_e P_e \quad (13)$$

Now let J_v dominate. Note that these operators commute with each other, hence they share common eigenspaces. Let $J_e \ll J_v$, with $J_v = 1$, and examine the corresponding perturbation theory where $H_0 = \sum_v P_v$ and $H' = \lambda \sum_e J_e P_e$, the perturbation Hamiltonian. Here, λ is a small factor to denote the perturbation order. Denote $|GS\rangle$ as the ground state of H_0 . As in Kitaev's paper [1], the effective Hamiltonian around the ground state is given by:

$$H_{\text{eff}} = T (H' + H' G'_0 H' + H' G'_0 H' G'_0 H' + \dots) T \quad (14)$$

where $T = |GS\rangle\langle GS|$ is the projector onto the ground state of H_0 , and $G'_0 = \left(\frac{1}{E_0 - H_0} \right)'$ is the Green's function, where the prime notation implies that G'_0 vanishes on the ground state and acts normally on the excited states.

Appendix A provides an explicit treatment of the perturbation method; here, we derive the effective Hamiltonian:

$$H_{\text{eff}} = (-1)^{\gamma_p} \sum_p \alpha_p \lambda^{l_p} W_p + \text{constant} \quad (15)$$

W_p is the plaquette operator, which is the product of check operators bordering the plaquette. l_p indicates the perturbation order and $(-1)^{\gamma_p}$ is used to fulfill the gap between the perturbed effective Hamiltonian with W_p . They are

explained in the appendix. α_p is an interesting path-dependent factor arises from the perturbation and we leave an interesting discussion of the zero point property in the appendix A.

When P_v is dominant, the two qubits placed on the vertex effectively become one qubit. The corresponding shrunken lattice, illustrated in Figure 4a, has $d_v = 4$, and the action of plaquette terms W_p around each vertex exerts the same local action on the vertex as in the toric code case, as shown in Figure 3.1.

Vertices with $d_v = 2k$ can be treated similarly, where $k > 2$ and k is an integer. Generally, for a vertex with an even d_v , we place $k = d_v/2 - 1$ qubits on the vertex, and designate $\otimes_k Z$, or P_{2k+1} , to be P_v and distribute the remaining d_v Pauli operators to the surrounding edges. The check operator is defined similarly to the case where $d_v = 4$. Then, the phase we are investigating is when all P_v s are dominant. We illustrate the example of a vertex with $d_v = 6$ in Diagram 4b. The computation is grounded on the mapping table to find the effective Hamiltonian, as in Table 1. Essentially, we provide a specific distribution of operators around the vertex and calculate the effective action of the plaquette terms on this vertex. We observe that the effective two qubits split into two connected vertices with $d_v = 4$. It is clear that both vertices maintain consistent and identical local properties as of the toric code. The generic mapping table for a vertex with degree $d_v \geq 4$ is shown in Appendix B. When we examine the ground state of dominant P_v s, each vertex with degree $d_v = 2k$ will split into $k - 1$ vertices with degree 4.

Operator	Effective operator
$X \otimes X \otimes 1$	$X \otimes 1$
$1 \otimes X \otimes X$	$1 \otimes X$
$1 \otimes 1 \otimes Z$	$1 \otimes Z$
$1 \otimes Z \otimes 1$	$Z \otimes Z$
$Z \otimes 1 \otimes 1$	$Z \otimes 1$

Table 1: Mapping Table for a vertex with $d_v = 6$

After splitting all vertices with $d_v = 2k$, we obtain the shrunken lattice. We conclude that a \mathbf{Z}_2 phase is recovered in the generalized Kitaev model with even degree vertices when the shrunken lattice is two-colorable.

3.3 Generalized model on arbitrary planar lattice

The remaining question concerns how to address vertices with an odd degree $d_v \geq 5$. It is logical to place $(d_v - 1)/2$ qubits on each vertex and distribute d_v Clifford operators to the surrounding edges so that all check operators are

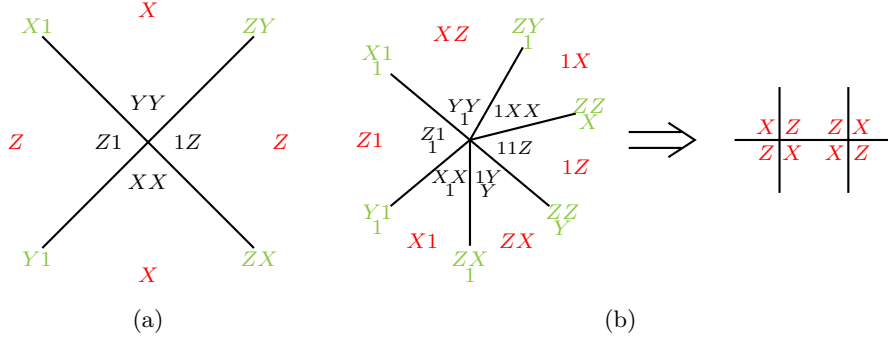


Figure 4: (a) Figure 1: This illustration demonstrates how the effective plaquette terms are obtained on the ground state of the P_e s. Each operator in the figure represents the action of either a check operator or a plaquette operator on the qubits located at the vertices. The green operator represents one of the anticommuting Clifford operators associated with edges. The black operator illustrates the plaquette term on a given vertex, and the red operator presents the effective plaquette term on the same vertex. (b) Figure 2: This depiction also shows how a vertex with degree $d_v = 6$ is transformed into two connected vertices, each with a degree of $d_v = 4$. It is essential to note that the effective action is consistent with the toric code case.

defined. The general Hamiltonian on a lattice $\Gamma = (V, E, P)$ is given by:

$$H = - \sum_{\{v|d_v=2k, k \in \mathbb{Z}\}} J_v P_v - \sum_{e \in E} J_e P_e, \quad (16)$$

$$P_e = P_{\partial_1 e} \otimes P_{\partial_2 e}. \quad (17)$$

We designate the stabilizer center S_c as H_0 , which includes all $\{P_v|v \in V\}$ and a subset S_e of $\{P_e|e \in E\}$ such that any two $P_e \in S_e$ commute with each other and with $\{P_v|v \in V\}$. In other words, S_e consists of check operators on the edges that connect vertices with an odd d_v . If we further require that the shrunk lattice at S_c is a two-colorable degree-4 lattice, or equivalently, that any two vertices with an odd degree are shrunk, then the effective Hamiltonian resembles the toric code model when the coefficients of S_c are dominant.

The proof involves transforming the lattice into one where all vertices have even degrees. Notably, if we make the operators on the edge connecting two vertices with odd degrees d_1 and d_2 dominant, it is algebraically equivalent to a single vertex with degree $d_1 + d_2 - 2$ and a dominant P_v . An example is illustrated in Figure 5, and the general case follows similarly. However, a vertex of odd degree cannot be made equivalent to the combination of two vertices with lower degree, thus making the generalization nontrivial.

We now conclude that on a general lattice Γ , if there exists a set S_c such that all vertices are shrunk and the resulting shrunk lattice is 2-colorable, the generalized Kitaev Spin liquid model resides in the \mathbf{Z}_2 phase.

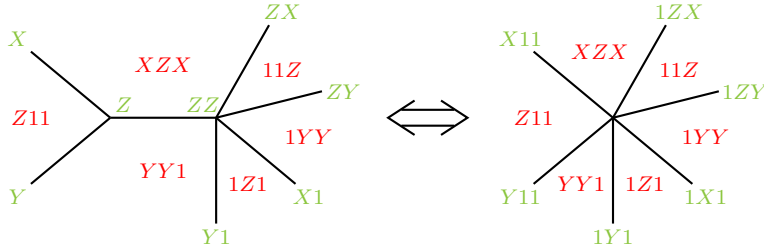


Figure 5: This illustration demonstrates that a vertex of degree 3 combined with a vertex of degree 5 is equivalent to a single vertex of degree 6. In the left above, a $P_e = Z \otimes Z \otimes Z$ over the red edge is put into the S_c , and in the right above, a $P_v = Z \otimes Z \otimes Z$ is put into the S_c . They have the same action of surrounding plaquette, hence these two cases are equivalent for our purpose.

4 Emergent Twist Defect in the gapped phase

In all previous instances, we selected S_c such that vertices with odd degrees were paired with each other, ensuring that any check operator would violate two terms in S_c . However, what happens if there is an odd-degree vertex, such as a trivalent vertex, that has not been paired with another odd-degree vertex? Revisiting the Honeycomb lattice, as depicted in Figure 7b, the effective Hamiltonian resembles a toric code model with two defects, similar to the findings in [4]. Notably, in our case, there is one additional plaquette as well as one more qubit within the defect line. This demonstrates that we can create a dislocation defect at the toric code level with a regular lattice at the spin liquid level! As studied in [15], this type of lattice dislocation defect could capture unpaired Majorana modes in the original Honeycomb model.

It's important to note that the lattice itself is regular and the lattice dislocation at the toric code level is due to a specific choice of S_c ! Remarkably, altering S_c is simpler than deforming the lattice itself. We will demonstrate in the following that a linearly interpolating Hamiltonian with different S_c choices can manipulate the defects.

The defect remains at the trivalent vertex, as a degree of three disrupts the local 2-colorability, as indicated in Figure 7a. Therefore, moving the defect involves relocating the trivalent vertex.

Consider Figure 8, which depicts a section of a larger lattice, similar to those shown in Figures 6 and 7. All check operators on yellow edges are designated as dominant. The configuration outside this localized area remains unchanged. This setup presents five potential configurations, where the effective Hamiltonian can represent the toric code, with or without defects. To transition between these static states, we introduce time evolution, facilitating the creation, movement, and fusion of defects.

Focusing on the movement of a defect as a detailed example (the other processes are analogous), we examine a more specific local structure in Figure 9,

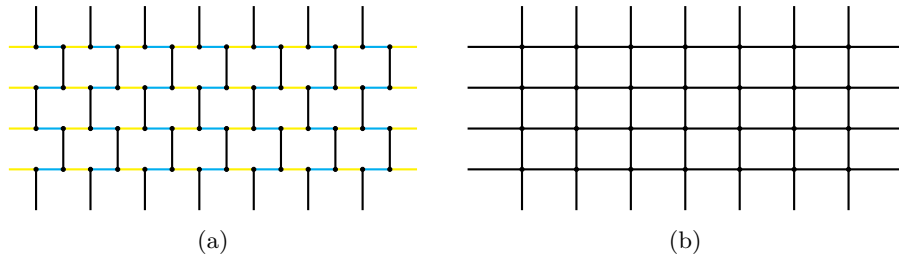


Figure 6: (a) Shows a honeycomb lattice where all vertices have been paired and shrunk by dominating the yellow edges. (b) The resulting effective or shrunk lattice where a toric code Hamiltonian acts.

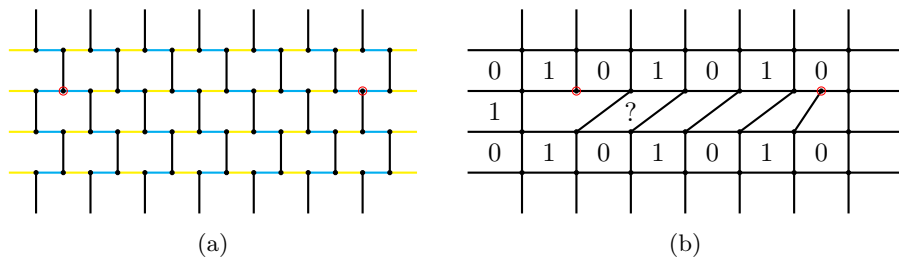
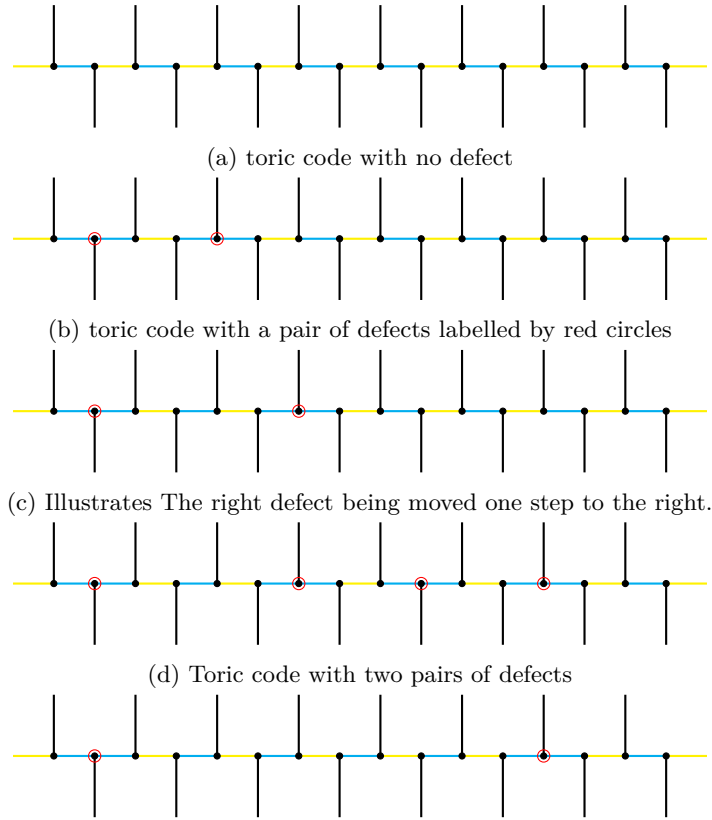


Figure 7: (a) Displays a situation where two trivalent vertices (labelled by red circles) are not shrunk with another vertex. (b) shows the underlined phase where all check operators on yellow edges are dominant. This represents the toric code with a pair of defects.



(e) Illustrates the process of fusing the two middle defects, which merges the separate pairs into a single pair.

Figure 8: The figures presented above depict the static Hamiltonian on a portion of the lattice. It is required that all check operators on yellow edges be dominant. Different choices of dominant check operators will lead to various cases of the effective toric code Hamiltonian, with or without defects.

which illustrates the transformation from Figure 8b to Figure 8c. We use $H(0)$ and $H(T)$ to denote their respective static Hamiltonians. The linear interpolation between them is introduced as follows:

$$H(t) = H(0) \left(1 - \frac{t}{T}\right) + H(T) \frac{t}{T} \quad (18)$$

$H(0)$ and $H(T)$ represents the Hamiltonian with dominant coefficients of $S_c(0)$ and $S_c(T)$ and all perturbation terms were shut down to avoid subtlety. $H(t)$ commutes with all the plaquette terms so the action of all plaquette terms remains unchanged. Therefore, the action of the time evolution operator on the stabilizer center S_c is crucial. We expect the state will transition into the spectrum of new stabilizer centers.

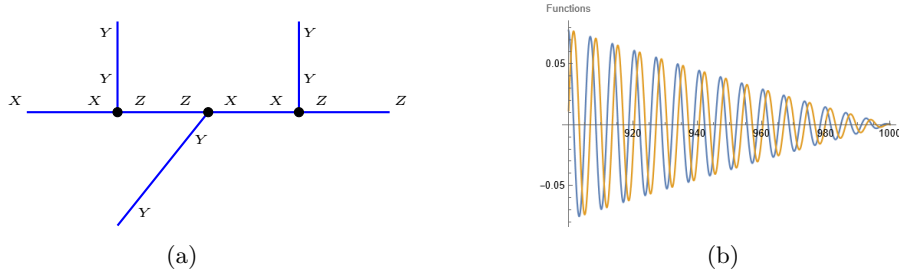


Figure 9: The figure on the left depicts a detailed local part of a honeycomb lattice to elucidate the movement of a defect, with the check operator explicitly labeled. On the right, the numerical results are displayed, illustrating that the real and imaginary differences between β_1 and β_2 vanish at $T = 1000$. Furthermore, this pattern persists for all $T > 1000$.

Note that most terms remain unchanged, contributing to a constant phase, as the state is always their eigenstate with an eigenvalue of $+1$. The only non-trivial terms are:

$$H = -\frac{t}{T} Z \otimes Z \otimes 1 + -(1 - \frac{t}{T}) 1 \otimes X \otimes X \quad (19)$$

The time evolution operator (TEO):

$$O(t) = \mathcal{T} \int e^{iH} dt \quad (20)$$

This is a formal notation; calculations need to be done by explicitly applying the Time Order operator \mathcal{T} . But we realize that after expanding $O(t)$, the general form is:

$$O(t) = a(t) + b(t) Z \otimes Z \otimes 1 + c(t) 1 \otimes X \otimes X + d(t) Z \otimes Y \otimes X \quad (21)$$

Where a, b, c , and d are complex, time-dependent functions. Since the operator $O(t)$ acts on the ground state of $1 \otimes X \otimes X$, a simplified representation is allowed

due to the trivial action of $1 \otimes X \otimes X$:

$$O(t) = \beta_1 + \beta_2 Z \otimes Z \otimes 1 \quad (22)$$

Utilizing the differential equation

$$\frac{dO(t)}{dt} = HO(t) \quad (23)$$

we numerically solve for $O(t)$, finding that at time T , $O(T) = \beta(1 + Z \otimes Z \otimes 1)$. Here, β is a complex number whose significance is determined by the value of T . Assuming the ground state initiates as

$$|GS\rangle_{t=0} = \prod_{p \in P} \frac{W_p + 1}{2} \bigotimes_{v' \in V'} |0\rangle_{v'} \quad (24)$$

Remember V' is the set of vertices on the shrunken lattice. Since the plaquette operators commute with the time evolution operator, the ground state transitions to:

$$|GS\rangle_{t=T} = \prod_{p \in P} \frac{W_p + 1}{2} \left\{ O(T) \bigotimes_{v' \in V'} |0\rangle \right\} \quad (25)$$

This is equivalent to the ground state of $H(T)$! Thus we claim we are able to move the defect.

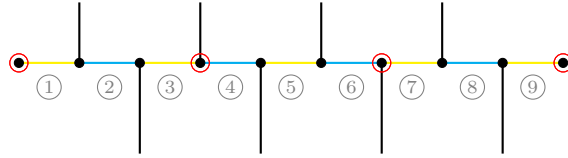


Figure 10: The image displays a local section of the lattice, where alternating red and blue edges represent the $X \otimes X$ and $Z \otimes Z$ checks respectively. Each edge is labeled by a unique number, with the check operator of the corresponding edge identified accordingly. The red circles indicate the positions intended for defect placement.

It is instructive to concentrate on a single chain as depicted in Figure 10. In this illustration, red edges correspond to the check operator $X \otimes X$, and blue edges to $Z \otimes Z$. These operators are denoted by Op_i , where i signifies the numerical assignment to the edges. Initially, all blue checks are designated as part of the Stabilizer center.

Within this framework, we explore several critical processes. The initial process entails the creation of defects via the application of the Hamiltonian:

$$H(t) = -(Op_1 + Op_3) \left(1 - \frac{t}{T}\right) - (Op_2) \frac{t}{T} \quad (26)$$

Terms that commute with $H(t)$ are omitted. A numerical solution reveals that the time evolution operator is expressed as:

$$O^{creation}(T) = \beta(T)(1 + Op_2) \quad (27)$$

This implies that the state will be projected onto the ground state of Op_2 , as anticipated, leading to the creation of a pair of defects. This transformation is represented in the transition from Figure 8a to Figure 8b.

In the second scenario, the movement of one of the defects is achieved through the following process:

$$H(t) = -(Op_2 + Op_5) \left(1 - \frac{t}{T}\right) - (Op_2 + Op_4) \frac{t}{T} \quad (28)$$

As explicitly demonstrated above, this time evolution is as expected to move defects.

The final process to consider is the fusion of defects. The initial case of fusion involves creating a pair of defects and subsequently fusing them back together, essentially reversing the creation process:

$$H(t) = -Op_2 \left(1 - \frac{t}{T}\right) - (Op_1 + Op_3) \frac{t}{T} \quad (29)$$

The numerical solution for the time evolution operator is given by:

$$O(T) = \beta_3(T)(1 + Op_1)(1 + Op_3) + \beta_4(T)[(1 - Op_1)(1 + Op_3) + (1 + Op_1)(1 - Op_3)] \quad (30)$$

In this scenario, only $(1 + Op_1)(1 + Op_3)$ has non-zero action by examining energy levels. This indicates that upon fusing the pair created from the vacuum, we algebraically regain the vacuum state as expected. A more intriguing case of fusion involves creating two pairs of defects from the vacuum, as depicted in Figure 8d, and then fusing the two central defects. Denote the state before fusion as $|GS_4\rangle$, derived from creating four defects from $|GS\rangle$, as seen in Equation 24. The process then transitions these two pairs into a single pair:

$$H(t) = -Op_5 \left(1 - \frac{t}{T}\right) - (Op_4 + Op_6) \frac{t}{T} \quad (31)$$

The TEO is similar as 30:

$$O(T) = \beta_5(T)(1 + Op_4)(1 + Op_6) + \beta_6(T)[(1 - Op_4)(1 + Op_6) + (1 + Op_4)(1 - Op_6)] \quad (32)$$

To check the fusion rule of the defects. We should check the normalization of the projectors. We will see $\langle GS_4 | (1 \pm Op_4)(1 \pm Op_6) | GS_4 \rangle$ is consistently identical. To understand this, notice that:

$$\langle GS_4 | Op_4 | GS_4 \rangle = \langle GS_4 | Op_6 | GS_4 \rangle = 0 \quad (33)$$

This is because $Op_4(Op_6)|GS_4\rangle$ has different energy from $|GS_4\rangle$, as $\frac{1+Op_5}{2}|GS_4\rangle = |GS_4\rangle$ and $Op_4\frac{1+Op_5}{2}|GS_4\rangle = \frac{1-Op_5}{2}Op_4|GS_4\rangle$. The intricate part is:

$$\langle GS_4|Op_4 \otimes Op_6|GS_4\rangle = \left(\bigotimes_{v' \in V'} \langle 0|_{v'} \right) \prod_{p \in P} \frac{W_p + 1}{2} Op_4 \otimes Op_6 \left(\bigotimes_{v'' \in V'} |0\rangle_{v''} \right) \quad (34)$$

Remember V' here represents the set of vertices of the shrunken lattice. Notice:

$$\left(\bigotimes_{v' \in V'} \langle 0|_{v'} \right) \prod_{p \in P'} W_p Op_4 \otimes Op_6 \left(\bigotimes_{v'' \in V'} |0\rangle_{v''} \right) = 0 \quad (35)$$

Because, for any $P' \subset P$, the product of W_p s always acts on a trivial loop of the lattice, which can not match the action of the $Op_4 \otimes Op_6$ on an open cut. And $Op_4 \otimes Op_6$ itself can not act trivially on $\bigotimes_{v \in V'} |0\rangle_v$.

Naturally, $(1 + Op_4)(1 + Op_6)$ yields the vacuum, while $(1 - Op_4)(1 + Op_6) + (1 + Op_4)(1 - Op_6)$ gives rise to a free fermion. If fusion rule obeys the rule of the Ising Anyon, their coefficients should satisfy:

$$\beta_5(T) = \sqrt{2}\beta_6(T) \quad (36)$$

Numerical solutions suggest that $|\beta_5(T)| = \sqrt{2}|\beta_6(T)|$, with a surprisingly introduced phase. However, we can account for this by moving the phase into the definition of the state or choose the T carefully to let the phase vanish. As highlighted in [1], the free fermion excitation exhibits the same algebra as the composite quasi-particle of electric and magnetic charge ϵ of the toric code, even though they differ in energy. Kitaev proposed that the free fermion would decay to ϵ when exposed to a certain thermal bath. Consequently, we can deduce that the defects explicitly comply with the nontrivial fusion rule of the Ising Anyon as demonstrated in [4]:

$$\sigma \times \sigma = 1 + \epsilon \quad (37)$$

σ represents the twist defect. ϵ represents the fermion. The last thing we have to care is that although the action of plaquette terms are fixed during time evolution, the effective Hamiltonian may flip its sign so it may have excitations which violates plaquette terms.

To see this, rewrite the overall Hamiltonian in a simplified manner:

$$H = -S_c - c_p W_p \quad (38)$$

c_p absorbs all coefficients of the plaquette operators and S_c are dominant. From explicit numerical evaluation in appendix(A.1), the sign of two plaquette operator flips after creating or fusing a pair of defects. So two extra excitations appear or annihilate but moving defects won't create any excitation as shown in diagram11. The yellow plaquette is the one that is excited while white plaquette stays at the ground state of the corresponding W_p . The overall picture is: create two pairs of defects and four plaquettes carry plaquette excitations. Then the central two defects fused with two plaquette excitation annihilates, leaving

a superposition of vacuum and free fermion excitation, which agrees with the picture that the defects capture the Majorana fermion and behaves like Ising anyon.

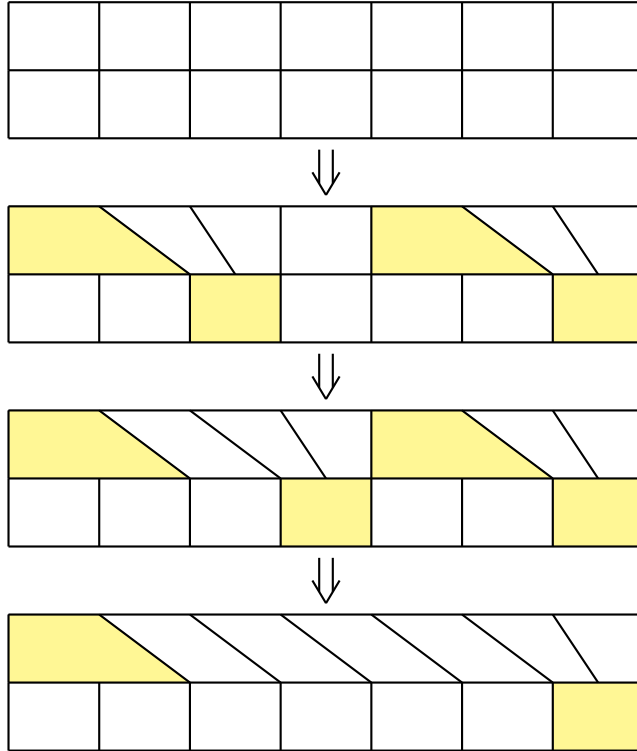


Figure 11: Demonstration of the excited plaquettes. Yellow plaquettes are the excited ones while white plaquettes stays at the ground state of the corresponding plaquette operators. The first figure is a part of regular surface code case and the state stays at the ground state. When two pairs of defects are created, two pairs of plaquettes, which have the trivalent vertex, will be excited. Moving defects will move the excited plaquettes accordingly with no more excitation created. After fusing the central two defects, the corresponding excitation annihilates, leaving two remaining defects at ends.

5 Subsystem Code aspects

In recent work of [16], the Kitaev spin liquid code on trivalent and 3-colorable lattice has been proved to be a zero-logical-qubit subsystem code. Here we generalize it to our case. We use some notations to describe the lattice by n_v , the number of vertices, n_e , the number of edges, n_p , the number of plaquettes. We only look at orientable lattice, which could be easily extended to non-orientable

cases. We would first prove it is true when all the vertices of lattice have odd degrees. The gauge group is generated by $P_e|e \in E$. So the number of gauge group generators is $n_e - 1$ due to the $\prod_{e \in E} P_e = 1$. Then the generators of stabilizer group S is generated by $\{W_p|p \in P\} \cup \{W_l\}$, where W_l denotes the set of operators that are formed by the product of check operators along non-trivial loops of the lattice. So the number of the generators of S is given by $n_p - 1 + k$, where k is the number of non-trivial loop on the lattice. Assume vertex v has degree d_v and t_v qubits are placed on it. Then:

$$n_v - n_e + n_p = 2 - k \quad (39)$$

$$2n_e = \sum_v d_v \quad (40)$$

$$n_q = \sum_v t_v \quad (41)$$

Where n_q is the number of total qubits. The number of logical qubit n_L of this subsystem code is given by

$$n_L = n_q - (n_g - n_s)/2 - n_s \quad (42)$$

$$= 1/2 (2n_q - n_g - n_s) \quad (43)$$

$$= 1/2 (2n_q - n_e - n_p + 2 - k) \quad (44)$$

$$= 1/2 (2n_1 - n_e + n_v - n_e) \quad (45)$$

$$= 1/2 (\sum_{v \in V} 2t_v + 1 - d_v) \quad (46)$$

In our setup, the number of qubit on an odd degree vertex is given by $t_v = (d_v - 1)/2$. So it will automatically let $n_L = 0$. An even degree vertex could be treated as two connected odd degree vertices as depicted in Fig. 5, but in a converse manner. Clearly, this splitting does not change any of the aforementioned total quantities. So our generalized two dimensional Kitaev spin liquid model is always a zero-logical-qubit subsystem. The implication of floquet code is possible but out of the scope of this paper.

6 Conclusion and outlook

In this paper, we have generalized the Kitaev spin liquid model on a general planar lattice. We proposed that if we can identify a stabilizer center S_c to satisfy certain requirement, that S_c contains maximum amount of commuting check operators, the vicinity of the ground state of S_c will be effectively toric code model. If a single trivalent vertex remains in the shrunken lattice, a pair of twist defects would emerge, exhibiting Non-Abelian statistics as Ising Anyons. We have conclusively shown that we can manipulate and fuse the defect as long as the Hamiltonian is altered slowly. Furthermore, the processes of creation, movement, and fusion are all achieved by the time evolution operator, which are inherently unitary operators. It is equivalent to say we can use unitary

operators to create, move and fuse defects, which aligns with our usual taste of manipulating anyons. Nonetheless, braiding continues to pose a challenge in this context. In conclusion, the generalized spin liquid model appears to be a versatile platform for realizing a general surface code.

Several promising directions for future research emerge from this study. For instance, the nature of a defect resulting from a left vertex of degree 5 remains to be explored. The algebra looks similar but it creates defect disrupting more plaquettes. An extension to describe three dimensional topological phases or Fractonic phases would also be an intriguing prospect, and is currently under preparation. An analytical calculation of the geometric factor α_p may be interesting since the numerical calculation yields highly regular and interesting results. Moreover, a more general and analogous generalization that could support the non-Abelian Kitaev Quantum Double model would be of significant interest and importance.

Acknowledgments.

The authors are partially supported by NSF CCF 2006667, Quantum Science Center (led by ORNL), and ARO MURI.

References

- [1] Alexei Kitaev. “Anyons in an exactly solved model and beyond”. In: *Annals of Physics* 321.1 (Jan. 2006). arXiv:cond-mat/0506438, pp. 2–111. DOI: 10.1016/j.aop.2005.10.005.
- [2] A. Yu Kitaev. “Fault-tolerant quantum computation by anyons”. In: *Annals of Physics* 303.1 (Jan. 2003). arXiv:quant-ph/9707021, pp. 2–30. DOI: 10.1016/S0003-4916(02)00018-0.
- [3] Michael A. Levin and Xiao-Gang Wen. “String-net condensation: A physical mechanism for topological phases”. In: *Physical Review B* 71.4 (Jan. 2005), p. 045110. DOI: 10.1103/PhysRevB.71.045110.
- [4] H. Bombin. “Topological Order with a Twist: Ising Anyons from an Abelian Model”. In: *Physical Review Letters* 105.3 (July 2010). arXiv:1004.1838 [cond-mat, physics:hep-th, physics:quant-ph], p. 030403. DOI: 10.1103/PhysRevLett.105.030403.
- [5] T. I. Andersen et al. “Non-Abelian braiding of graph vertices in a superconducting processor”. In: *Nature* (May 11, 2023). ISSN: 1476-4687. DOI: 10.1038/s41586-023-05954-4. URL: <https://doi.org/10.1038/s41586-023-05954-4>.
- [6] Huaixiu Zheng, Arpit Dua, and Liang Jiang. “Demonstrating non-Abelian statistics of Majorana fermions using twist defects”. In: *Physical Review B* 92.24 (Dec. 2015), p. 245139. DOI: 10.1103/PhysRevB.92.245139.

- [7] Yi-Zhuang You and Xiao-Gang Wen. “Projective non-Abelian Statistics of Dislocation Defects in a Z_N Rotor Model”. In: *Physical Review B* 86.16 (Oct. 2012). arXiv:1204.0113 [cond-mat, physics:quant-ph], p. 161107. DOI: 10.1103/PhysRevB.86.161107.
- [8] Victor Chua, Hong Yao, and Gregory A. Fiete. “Exact chiral spin liquid with stable spin Fermi surface on the kagome lattice”. In: *Physical Review B* 83.18 (May 2011), p. 180412. DOI: 10.1103/PhysRevB.83.180412.
- [9] Congjun Wu, Daniel Arovas, and Hsiang-Hsuan Hung. “ Γ -matrix generalization of the Kitaev model”. In: *Physical Review B* 79.13 (Apr. 2009), p. 134427. DOI: 10.1103/PhysRevB.79.134427.
- [10] Hong Yao, Shou-Cheng Zhang, and Steven A. Kivelson. “Algebraic spin liquid in an exactly solvable spin model”. In: *Physical Review Letters* 102.21 (May 2009). arXiv:0810.5347 [cond-mat], p. 217202. DOI: 10.1103/PhysRevLett.102.217202.
- [11] Gino Cassella et al. “An Exact Chiral Amorphous Spin Liquid”. In: (Aug. 2022). arXiv:2208.08246 [cond-mat]. URL: <http://arxiv.org/abs/2208.08246>.
- [12] Shinsei Ryu. “Three-dimensional topological phase on the diamond lattice”. In: *Physical Review B* 79.7 (Feb. 2009). arXiv:0811.2036 [cond-mat], p. 075124. DOI: 10.1103/PhysRevB.79.075124.
- [13] Tim Eschmann et al. “Thermodynamic classification of three-dimensional Kitaev spin liquids”. In: *Physical Review B* 102.7 (Aug. 2020). arXiv:2006.07386 [cond-mat], p. 075125. DOI: 10.1103/PhysRevB.102.075125.
- [14] Matthew B. Hastings and Jeongwan Haah. “Dynamically Generated Logical Qubits”. In: *Quantum* 5 (Oct. 2021). arXiv:2107.02194 [quant-ph], p. 564. DOI: 10.22331/q-2021-10-19-564.
- [15] Olga Petrova, Paula Mellado, and Oleg Tchernyshyov. “Unpaired Majorana modes on dislocations and string defects in Kitaev’s honeycomb model”. In: *Phys. Rev. B* 90 (13 Oct. 2014), p. 134404. DOI: 10.1103/PhysRevB.90.134404. URL: <https://link.aps.org/doi/10.1103/PhysRevB.90.134404>.
- [16] Christophe Vuillot. “Planar Floquet Codes”. In: arXiv:2110.05348 (Dec. 2021). arXiv:2110.05348 [quant-ph]. URL: <http://arxiv.org/abs/2110.05348>.

A Perturbation treatment

A.1 Effective Hamiltonian

In this appendix, V represents the perturbation H' to avoid confusion. For the effective Hamiltonian as follows:

$$H_{eff} = T(V + VG'_0V + VG'_0VG'_0V + \dots)T \quad (47)$$

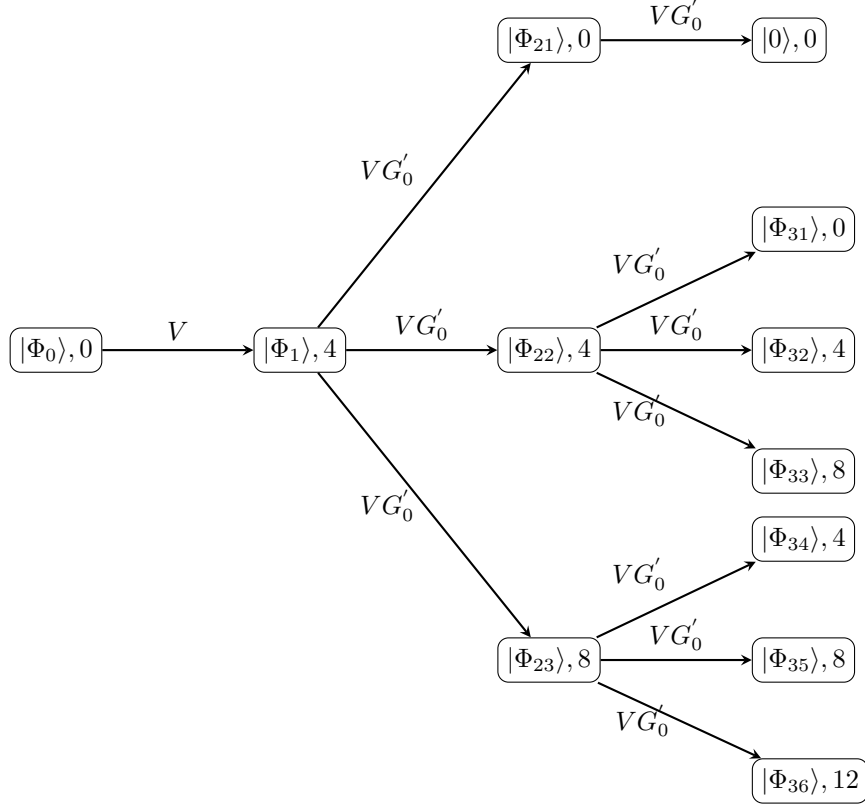


Figure 12: Demostration of perturbation tree

Where, $T = |GS\rangle\langle GS|$ is the projector onto the ground state of J_v s, and $G'_0 = (1/(E_0 - H_0))'$, where the prime notation implies G'_0 vanishes on the ground state and acts normally on the excited states.

The perturbation tree, shown in figure12, demonstrates the general idea of calculation. Each node of the diagram is labeled with a state Φ . The action of each check operator on $|\Phi_0\rangle = |GS\rangle$ will flip two terms in H_0 , which increases the energy by 4. Then, when we apply another term in V on the intermediate state $|\Phi_1\rangle$, different outcomes appear due to the product of $P_{e_1} \times P_{e_2}$, where:

If $\partial e_1 \cap \partial e_2 = \emptyset$, then we obtain $|\Phi_{23}\rangle$ with energy 8. If $\partial e_1 = \partial e_2$, then we obtain $|\Phi_{21}\rangle$, which goes back to the ground state. The remaining possibility is that e_1 and e_2 share one common order vertex and will have energy 4. If we repeat this process to achieve higher order perturbation, we obtain different sectors with different energy levels as shown in Figure 12. The energy sector $\Phi_{i,j}$ that reverts back to the ground state will contribute to the i th order of the effective Hamiltonian. Note that in the diagram, G'_0 always gives some constant factor.

Thus, we conclude:

$$H_{eff}^i = \alpha_i \langle GS | V^i | GS \rangle \quad (48)$$

Where α_i is a path-dependent factor calculable from the diagram. We name it the geometric factor. Consider the order of λ first. Terms in V^i that do not vanish in the ground state are those that commute with all P_v . Generators could be $P_{e_i} P_{e_j}$, where $e_i = e_j$, contributing to a constant factor, or $\Pi_{e_j} P_{e_j}$, where e_j forms a closed loop, contributing to the plaquette term $W'_p = \Pi_{e \in Bo(p)} P_e$. So we could conclude, the effective Hamiltonian is:

$$H_{eff} = \sum_p (-1)^{\gamma_p} \alpha_{l_p} \lambda^{l_p} W_p + constant \quad (49)$$

Where l_p is the number of edges that appears in W'_p . The factor λ^{l_p} arises from the dominant contribution in the l_p th order perturbation. We have to pay extra attention to the plaquette operators $W_p = \Pi_{e \in Bo(p)} P_e$. But the perturbation will end in W'_p , an incomplete form of the W_p . But we can recover W_p by adding the dominant check operators. To understand this, look at a special case as figure13. A plaquette consists of 6 edges and the check operators attached to them are labeled by A, B, C, D, E, F . Consider B, D is dominant as shown in the right above case, then A, C, E, F are perturbation terms. Numerical calculation shows that the perturbation gives $W'_p = \alpha_p ACEF = -\frac{1}{16} ACEF$. We can easily recover W_p by adding B and D by $W'_p BD = -\frac{1}{16} ACEFBD = -\frac{1}{16} ABCDEF$, since the state is the ground state of B and D with eigenvalue $+1$. This means the effective Hamiltonian can be written as $H_{eff} = -\frac{1}{16} W_p$. By this, the effective Hamiltonian could be fanalized to form15.

After the process of moving defects, it becomes the case that B and E are dominant, and we will get the exact same effective Hamiltonian by the same way. Since the action W_p remains invariant during time evolution. Combined with the fact that the state is the ground state of the dominant $S_c(T)$, we conclude it will ends in the ground state of the $H(T)$.

The cases of creation or fusion cases are different. In these cases, the plaquette will be transformed into cases(reversely for fusion process) that only D is dominant. The perturbation method gives $-\frac{1}{16} ABCFEF$. So $H_{eff} = -\frac{1}{16} ABCFEFD = \frac{1}{16} ABCDEF$. Thus, though W_p remains the same eigenvalue, it ends in excitation state since the different sign of the plaquette operator in the effective Hamiltonian.

A.2 Geometric Factor α_p

The geometric factor α_p needs to be evaluated via explicit calculation and we did not find a general formula for it. However, we generally only care about the cases that has factor $\alpha_p = 0$ since it will serve as a hole in the surface code limit. We find a family of plaquettes that would have $\alpha_p = 0$ when the corresponding plaquette operator consists of odd number of anti-commutative check operator pairs. The proof is as follows:

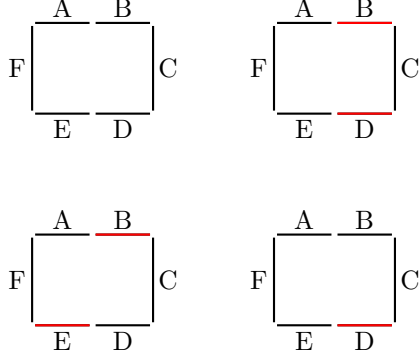


Figure 13: The figures above display a plaquette with 6 edges, where the red edges represent the dominant check operators and the black edges denote the perturbation terms. The figure in the top-right position illustrates a common scenario in the honeycomb lattice. The figure in the bottom-left position shows the case after moving defects, and the figure in the bottom-right position depicts the situation when there is a defect

Suppose we have a plaquette operator W'_p , which is a product of several perturbation check operators. So the factor α_p is calculated in the l_p th order of perturbation through the diagram(12). It is easy to tell that for any permutation $\sigma \in S_{l_p}$, the $\Pi_i A_{\sigma(i)}$ has a nontrivial perturbation contribution to the plaquette operator W'_p , where S_n is n th order of permutation group.

The perturbation contribution consists of two parts. One comes from the action of green function, which essentially comes from path on the perturbation tree, denoted as Fg_σ . Then the outcome of the perturbation could be written as $\alpha_p W'_p = \sum_{\sigma \in S_{l_p}} Fg_\sigma \Pi_i A_{\sigma(i)}$. So $\alpha_p = \sum_{\sigma \in S_{l_p}} Fg_\sigma Sg_\sigma$, where Sg_σ comes from making $\Pi_i A_{\sigma(i)}$ to a fixed form $W'_p = \prod_{i=1}^{l_p} A_i$, which is controlled simply by the commutation relation between A_i s. Consider $\bar{\sigma} : \bar{\sigma}(i) = \sigma(l_p - i + 1)$, a function that is the reverse permutation of σ . Notice that reverse the order of check operators in the perturbation tree still remains in the tree since it starts at the ground state and also ends at the ground state! And they have $Fg_\sigma = Fg_{\bar{\sigma}}$ due to the symmetry.

The relative sign $\frac{Sg_\sigma}{Sg_{\bar{\sigma}}}$ is determined by making $\Pi_i A_{\sigma(i)}$ to $\Pi_i A_{\bar{\sigma}(i)}$. To illustrate this, look at a simple example. Consider 3 elements A_1, A_2, A_3 , and $\sigma(i) = i$, $\bar{\sigma}(i) = 3 - i$. To make the product $A_1 \cdot A_2 \cdot A_3$ to $A_2 \cdot A_2 \cdot A_1$, we can swap A_1 with A_2 , then A_1 with A_3 , then swap A_2 with A_3 . The relative sign is decided by the commutation relation of A_i s. The general relative sign is done by the same way. We conclude the relative sign is given by the parity of the anti-commutative pairs. The relative sign is -1 if W'_p contains odd number of anti-commutative pairs of check operators, and $+1$ if even. That results in $\alpha_{l_p} = 0$ since the reverse permutation is an equivalence relation in the permutation group S_{l_p} .

Remark 1: In a general lattice with vertices that $d_v = 4$, we should note that the coefficient of each W_p is no longer uniform. But continuously deform the coefficients of W_p s to be uniformly large, regardless of the sign (as we have argued, the sign does not matter regarding the toric code phase). It is a continuous transformation which does not close the gap. Therefore, it will stay in the same phase.

Remark 2: One may worry about some unfortunate occasions that $\alpha_p = 0$. The factor is a path-dependent factor and depends heavily on the details of the lattice and the choice of S_c . But we argue that, for a zero α_p which have multiple channel in the diagram12, we can probably find a nonzero $l_p + 2$ th order contribution by insert a pair of P_{e_0} in the process to build up W_p , where $e_0 \notin Bo(p)$ into the perturbation tree, which will change the action of G'_0 between the pair of P_{e_0} . Since the action is generally non-linear, it might be nonzero. If it's still zero, we could insert more. Finally W_p may survive in higher order of perturbation theory.

Remark 3: if there is huge plaquette in the lattice Γ , since l_p is large, λ^{l_p} is generally so small that this plaquette could be treated as a hole or a boundary, of which the type depends on the color of it. Or, if some $\alpha_p = 0$, and could not survive even under the argument of remark 2, or it only survive in really high order perturbation, it also serves as a hole in the toric code model.

B Mapping Table of vertex with $d_v > 4$

Consider a vertex has degree $d_v > 4$. Let us assume $d_v = 2k$, so there are k qubits placed on it. We call an operator a k -order Pauli operator if it is a tensor product of k Pauli operators. We insist choosing $P_v = \bigotimes_k Z$, since the k qubits would stay on the ground state of P_v , with eigenstate of $+1$, without loss of generality, the eigenspace would be 2^{k-1} dimensional. So we have to find the effective $k-1$ order Pauli operators of those k order Pauli operators commuting with P_v . The generators of these k order are of following form:

$$\mathcal{X}_i = \underbrace{1 \otimes 1 \cdots 1}_{i-1} \otimes X \otimes X \otimes 1 \otimes \cdots 1 \otimes 1 \quad (50)$$

Here \mathcal{X} represents a tensor product of k pauli operator. \mathcal{X}_i is explicitly two X operator at position i and $i+1$, identity 1 at the others. We have obviously $k-1$ such operator $\{\mathcal{X}_i | i = 1, 2 \dots k-1\}$. Another set of generators are:

$$\mathcal{Z}_i = \underbrace{1 \otimes 1 \cdots 1}_{i-1} \otimes Z \otimes 1 \cdots 1 \otimes 1 \quad (51)$$

Which means \mathcal{Z}_i is one Z operator locates at position i , Identity 1 at the others. We have k such operators, $\{\mathcal{Z}_i | i = 1, 2, \dots, k\}$. Notice, $|\phi_0\rangle = \bigotimes_k |0\rangle$ is one of the basis in the eigenspace. $\mathcal{X}_i |\phi_0\rangle$ effectively generate the whole eigenspace.

Then we define the mapping of \mathcal{X}_i to $k - 1$ order operator:

$$\mathcal{X}_i \rightarrow \underbrace{1 \otimes 1 \cdots 1}_{i-1} \otimes X \otimes X \otimes 1 \otimes \cdots 1 \otimes 1 \quad (52)$$

We denote the notation $\tilde{\mathcal{X}}_i$ to represent the effective action of \mathcal{X}_i in the eigenspace of P_v . Notice on the right, it is a tensor product of $k - 1$ Pauli operators. Similarly, $\tilde{\mathcal{Z}}_i$ to represent the effective operator of \mathcal{Z}_i :

$$\tilde{\mathcal{Z}}_i = \underbrace{1 \otimes 1 \cdots 1}_{i-2} \otimes Z \otimes Z \otimes 1 \otimes \cdots 1 \otimes 1 \quad (53)$$

For $1 < i < k - 1$, and $\tilde{\mathcal{Z}}_1 = Z \otimes 1 \cdots 1 \otimes 1$, $\tilde{\mathcal{Z}}_k = 1 \otimes 1 \cdots 1 \otimes Z$. Notice the product of $\tilde{\mathcal{Z}}_i$ is 1, which agree with $\prod_{i=1}^k \mathcal{Z}_i = P_v$. Then arranging the operators similarly as in 4b would give rise to the splitting of $d_v > 6$.

C Possible Measurement-Based Initializing Method

We have emphasized that since each process is described by time evolution, which is natural to depict each process (movement, creation and fusion) by quantum circuit. Here we put down a convenient measurement-based method to initialize a ground state of the effective toric code on a honeycomb lattice as in figure 14, which is actually the same way as in the Floquet code in [14]. The method is to follow a measurement schedule:

- Step 1: Measure the check operators associated with yellow edges.
- Step 2: Measure the check operators associated with blue edges.
- Step 3: Measure the check operators associated with red edges.
- Step 4: repeat step 1.

After step 4, the state is the ground state of all plaquette terms (with signs that depend on measurement outcomes). We then proceed to measure the yellow checks (or equivalently the elements in S_c) as depicted in fig 6. Following this measurement, the state would transition into the ground state of the plaquette operators and the stabilizer center S_c (still the corresponding eigenvalues depend on the measurement outcome), thereby generating the effective toric code we want. Then we can apply the unitary operator which is given by the time evolution operators in previous section, to manipulate the twist defects.

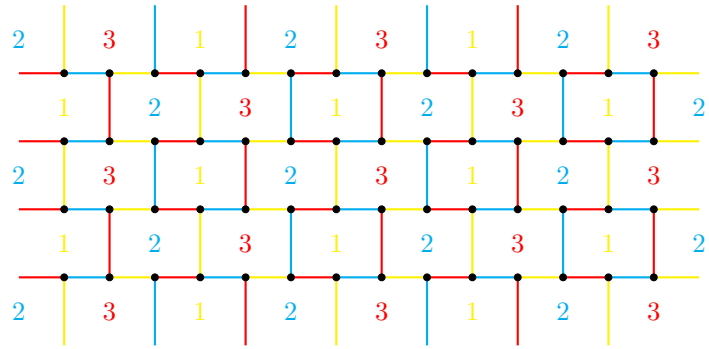


Figure 14: This figure illustrates a honeycomb lattice used to initialize a ground state of the effective toric code, a platform that facilitates defect manipulation. Each edge is colored according to the plaquettes to which it is connected.